UDK 621.791:669.14
Original scientific article/Izvirni znanstveni članek

ISSN 1580-2949
MTAEC9, 48(1)15(2014)

RELATIONSHIP BETWEEN A BAINITIC STRUCTURE AND THE HARDNESS IN THE WELD ZONE OF THE FRICTION-STIR WELDED X80 API-GRADE PIPE-LINE STEEL

ODVISNOST MED BAINITNO MIKROSTRUKTURO IN TRDOTO V PODROČJU ZVARA PRI TORNO VRTILNEM VARJENJU JEKLA X80 API ZA CEVOVODE

Hakan Aydin

Uludag University, Faculty of Engineering and Architecture, Department of Mechanical Engineering, 16059 Gorukle-Bursa, Turkey
hakanay@uludag.edu.tr

Prejem rokopisa – received: 2013-01-03; sprejem za objavo – accepted for publication: 2013-04-24

The present study focuses on the morphology of the weld zone, especially on the quantitative microstructural characterization of bainitic structures, and the relationship between post-weld bainitic structures and the hardness at the weld zone of the friction-stir welded X80 API-grade pipe-line steel. The employed rotating and traverse speeds of the polycrystalline cubic boron nitride tool during the friction-stir welding process were 350 r/min and 12.7 cm/min (5 inch per minute), respectively. A microstructural analysis of the weld was carried out using optical microscopy, orientation imaging microscopy and transmission electron microscopy, and the hardness variation was also mapped across the weld-plate cross section. The frictional heat and plastic flow during friction-stir welding create a granular bainitic structure (the stir zone), a lath-like upper bainitic structure (the hard zone) and a recrystallized equiaxed polygonal ferritic structure (the heat-affected zone) in the weld zone. The maximum hardness was observed in the classical upper bainitic microstructure in the hard zone. The minimum hardness was found in the heat-affected zone. A good correlation between the post-weld bainitic structures and the hardness in the weld zone was obtained; the hardness increases almost linearly with the decreasing bainite-lath and packet sizes.

Keywords: friction-stir welding, X80 steel, bainite, microhardness

Študija obravnava morfologijo področja zvara, posebno kvantitativno karakterizacijo bainitne mikrostrukture in odvisnost med bainitno strukturo po varjenju in trdoto zvara pri torno vrtilnem varjenju X80 API jekla za cevovode. Uporabljene hitrosti rotacije in prečne hitrosti orodja iz kubičnega bor nitrida med torno vrtilnim varjenjem so bile 350 r/min in 12,7 cm/min (5 inčev na minuto). Mikrostruktura zvara je bila pregledana s svetlobnim mikroskopom, z mikroskopijo usmerjenosti slik in s presevno elektronsko mikroskopijo. Prikazano je spreminjanje trdote po prečnem prerezu zvara. Toplota zaradi trenja in plastični tok materiala med torno vrtilnim varjenjem povzročita nastanek zrnate bainitne strukture (cona mešanja), latasti zgornji bainit (trda cona) in rekristalizirano poligonalno feritno strukturo (toplotno vplivana cona) v zvaru. Najvišja trdota je bila opažena v navadni mikrostrukturi gornjega bainita v trdi coni. Najnižja trdota je bila v toplotno vplivani coni. Ugotovljena je bila dobra korelacija med bainitno strukturo zvara in trdoto v coni zvara: trdota narašča skoraj linearno z manjšanjem bainitnih lat in velikostjo bainitnega sestava.

Ključne besede: torno vrtilno varjenje, jeklo X80, bainit, mikrotrdota

1 INTRODUCTION

The commercial high-strength low-alloy (HSLA) type X80 API-grade (American Petroleum Institute) steels produced with thermo-mechanically controlled processing (TMCP), which produces uniformly refined microstructures consisting of ferrite and bainite, are typically used in several oil and gas operations. The high strength, good toughness and excellent corrosion resistance of the X80 steel are obtained with chemical composition design, controlled rolling and controlled cooling. Welding is the essential process for large-scale pipelines for a long-distance transportation of crude oil or natural gas under a high pressure. A large heat input in the conventional fusion-welding processes such as the arc and laser-beam welding alters the microstructure, deteriorates the mechanical properties, promotes solidification cracking and expedites hydrogen embrittlement in the weld zone. For the pipeline industry in particular, friction-stir welding (FSW) is a promising technique that has several advantages over the conventional fusion-welding processes, due to its low heat input and absence of the melting and solidification process.[1,2] Compared to the conventional fusion-welding methods, the advantages of the FSW process include better mechanical properties, a low residual stress and distortion, and a reduced occurrence of defects.[3,4] FSW is also a "green technology" as it produces no arc radiation, no fumes and no hazardous waste. In addition, in the case of steels, it is expected that hydrogen-induced cracking is severely reduced.

FSW is a solid-state materials-joining process invented by TWI in 1991, which is presently attracting a considerable interest and has been extensively developed for aluminum alloys, as well as for magnesium, copper, titanium and steel.[1–5] The FSW process utilizes a non-consumable tool that is inserted into the abutting edges of the base metal. In this process, a cylindrical tool is rotated and traversed along a square-butt weld joint similar to the milling technique.[2] The joined material is

plasticized by the heat generated by the friction between the surface of the plates and the contact surface of a special tool, composed of two main parts: a shoulder and a pin.[6]

FSW has recently become an attractive process for joining HSLA-type steels.[7–11] However, it is very difficult to friction-stir weld on HSLA-type steels due to their high strength and high-heat-input demands for adequate welding. An interest in using this process to join steels has become popular due to the advancements in the friction-stir-welding tool development. Currently, the tool pins used such as polycrystalline boron nitride (PCBN) have been successful in welding HSLA-type steels.[7,10–12]

The microstructure and mechanical properties of friction-stir welds are dependent on the chemical composition and the microstructure of the base metal, the thermo-mechanical conditions during the FSW process and the cooling rate to room temperature. As mentioned above, the FSW process affects the material not only thermally but also mechanically. An understanding of the microstructural evolution during the FSW process and the mechanisms, with which the associated microstructures affect the mechanical and physical properties such as strength, fatigue, creep and corrosion, is critical.[13] So, the morphology of the weld zone for friction-stir welds need to be characterized.

The bainitic structures formed at the weld zone are the primary factor affecting the post-weld properties of FSWed X80 steels. Therefore, it is vital to carry out a characterization of the bainitic structures acquiring quantitative data in the weld zone in order to develop a more fundamental understanding of the FSW process in X80 steels. Although there are several studies on the microstructure and mechanical properties of FSWed HSLA steels, especially of the HSLA 65 steel, in the literature,[10–12,14] only a few limited studies focused on the microstructure and properties of the FSWed X80 steel.[15–18] The present study focuses on the morphology of the weld zone, especially on the quantitative microstructural characterization of bainitic structures and the relationship between the post-weld bainitic structures and the hardness at the weld zone in the FSWed X80 API-grade pipe-line steel.

Figure 1: RM-2 model FSW machine[19]
Slika 1: Model RM-2 stroja za FSW[19]

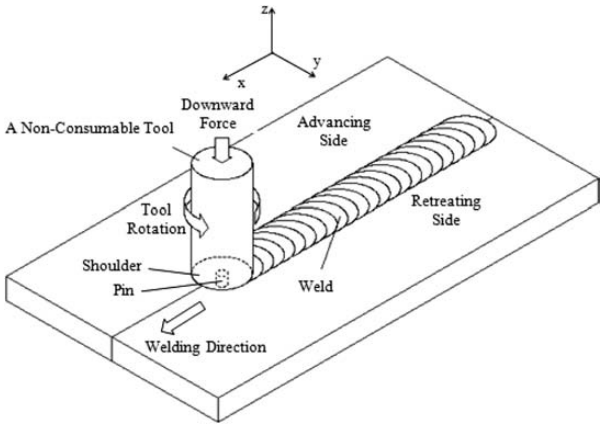

Figure 2: Schematic illustration of the FSW process
Slika 2: Shematski prikaz FSW-procesa

2 EXPERIMENTAL DETAILS

The material used in this work was a commercial API X80-grade pipe-line steel plate with a thickness of 11 mm, whose chemical composition (mass fractions, *w*/%) is listed in **Table 1**. The test plate was friction-stir welded longitudinally parallel to the rolling direction in the bead-on-plate configuration using a modified MTI RM-2 FSW machine built with the stiffness and spindle characteristics designed specifically for the FSW of steels, including a full data acquisition and display capability (**Figures 1** and **2**).[19] This equipment uses servo-controlled axes and a variable frequency drive on the spindle, with the speed range of up to 1800 r/min and the motor torque of up to 550 N m. A polycrystalline cubic boron nitride (PCBN) CS4 tool was used for the weld

Table 1: Chemical composition (*w*/%) of the X80 steel used in this investigation
Tabela 1: Kemijska sestava (*w*/%) jekla X80, uporabljenega v tej preiskavi

Fe	C	Si	Mn	S	P	Ni	Cr	Cu	Ti	Mo	Nb	N	Al	V
Balance	0.04	0.135	1.7	0.001	0.013	0.147	0.41	0.263	0.014	0.005	0.102	0.006	0.031	0.002

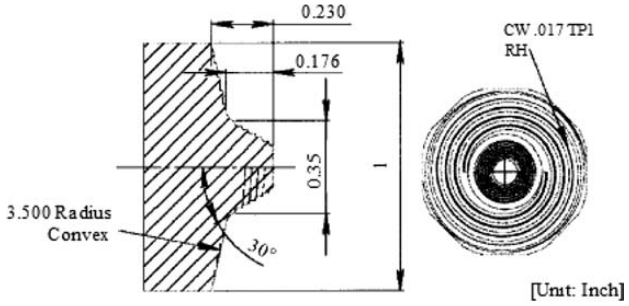

Figure 3: Geometry of the CS4 tool used in the welding[10,11]
Slika 3: Geometrija orodja CS4, uporabljenega pri varjenju[10,11]

(**Figure 3**). The employed rotating and traverse speeds of the tool during the FSW process were 350 r/min and 12.7 cm/min (5 inch per minute), respectively. All the welds were performed in the partial-penetration mode using a depth-controlled process (**Figure 4**). The tilt degree of the stir pin relative to the work-piece was set equal to 0.5° during the plunge and welding process. An argon gas atmosphere, at a flow rate of 1.1 m^3/h, was used, as the shielding gas, to prevent a surface oxidation during the weld cycle and to prolong the tool life. The shielding-gas flow is realized by means of the canals in the tool holder (**Figure 5**).[20]

After welding, the FSW sample was cross-sectioned perpendicularly to the welding direction using a water-jet cutter for microstructural examinations and micro-hardness measurements. An Olympus GX51 microscope was used for optical observation. Orientation-imaging-microscopy (OIM) examination was carried out using an FEI XL-30 SFEG. The scan-step size was 0.15 μm. An electron beam of 25 kV and a spot size of 5 were used with a specimen working distance of 14 mm and a specimen tilt angle of 70°. The electron-backscatter-diffraction (EBSD) data was collected and analyzed with TSL OIM Data Collection version 5.2 and OIM Analysis version 5.2, respectively. The crystallographic data was expressed as an inverse pole figure (IPF) with image quality (IQ) maps and grain-boundary (GB) maps. Transverse samples for transmission-electron-microscopy (TEM) studies were prepared by cutting 3-mm-diameter cylinders with an electrical discharge

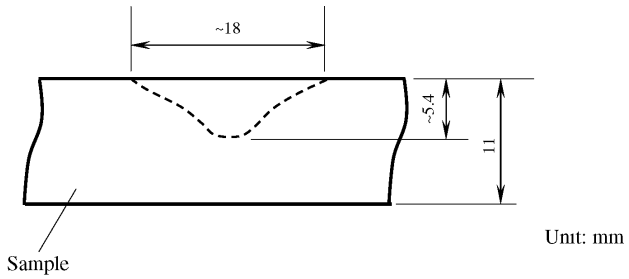

Figure 4: Partial-penetration mode (the FS weld nugget indicated with a dashed line)
Slika 4: Način delne penetracije (jedro FS-zvara je prikazano s črtkano linijo)

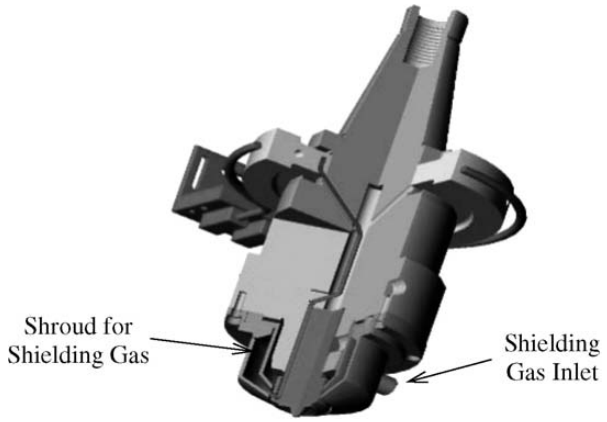

Figure 5: Shielding-gas flow in the tool holder[20]
Slika 5: Pretok varovalnega plina v nosilcu orodja[20]

cutting machine (EDM) from the selected areas of the sample. The electron-transparent thin sections for the TEM analysis were prepared by means of double jet electro-polishing, using a solution of 10 % (volume fraction) perchloric acid and 90 % glacial acetic acid with 25 V below 0 °C in the icy water. These thin foil specimens were examined with a Philips FEG model transmission-electron microscope at 300 kV to observe the microstructural details. In order to identify different zones in the weld region to be scanned in the OIM examinations and establish a correlation between the hardness and the post-weld bainitic structure, the hardness variation was mapped across the weld-plate cross-section using a LECO LM 100AT microhardness tester and the Amh43 version software using a diamond pyramid indenter with a load 500 g, dwell time 15 s and a indent spacing (vertical and horizontal) 400 μm. The microhardness map for the FSW sample was obtained with approximately 1800 and 1200 hardness indents in horizontal and vertical directions, respectively.

3 RESULTS AND DISCUSSION

The hardness map is a direct indicator of a microstructural evaluation during the FSW process. The hardness map of the FSWed X80 steel shows several features in the weld zone (**Figure 6**): the softening on both sides of the weld, the heat-affected zone (HAZ); almost the same hardness of the weld nugget as that of the base metal (BM), the stir zone (SZ); and the hardest region, the hard zone (HZ) within the advancing side (AS) of the weld zone, where the high temperature and strain were applied. The post-weld microstructures in the weld zone are influenced greatly by the peak temperature, the level of deformation and the local cooling rate to room temperature during the FSW process. The non-uniform distribution of hardness correlates to the non-uniform strain and heat gradient generated in the weld zone. The higher stresses on the AS of the weld result in an asymmetric heat generation across the SZ.

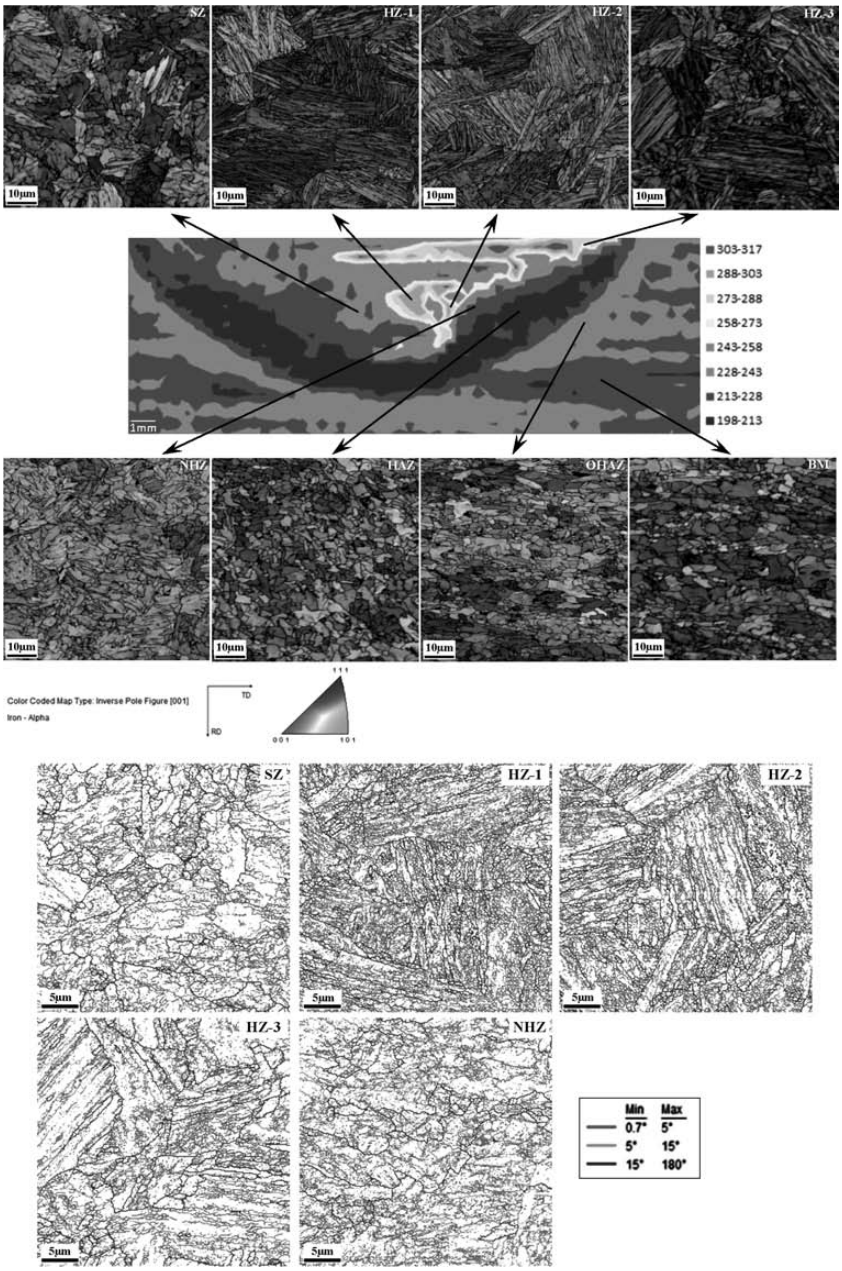

Figure 6: IPF with IQ and GB maps of various FSW zones (SZ: stir zone; HZ: hard zone; NHZ: near-hard zone; OHAZ: outer heat-affected zone)

Slika 6: IPF z IQ- in GB-prikazom različnih področij FSW (SZ: področje mešanja, HZ: trdo področje, NHZ: toplotno vplivano področje, OHAZ: izven toplotno vplivanega področja)

The hardness peaks commonly follow a line on the AS of the weld close to the location of the shoulder and the edge of the weld tool. This is due to a greater amount of the material shearing in this region, leading to a higher strain and greater heating, thereby resulting in a re-austenitization and subsequent transformation to a completely lath-bainitic microstructure during the FSW process.[10] That is, the strain rate and the peak temperature in the weld zone play a key role in the re-austenitization during the FSW process.

The BM microstructure is mainly composed of elongated fine-grained polygonal ferrites, with the average grain size of 6.09 μm, and a small amount of refined upper-bainite islands (**Figures 6** and **7**). There is no evidence of the BM microstructure in the SZ and HZ regions (**Figure 6**). The elongated grains in the BM have completely transformed to a bainitic microstructure with well-defined lath-like upper bainite, consisting of thin, relatively straight and long, parallel ferrite laths in the HZ regions. This microstructure indicates that the BM has reached the peak temperature in excess of A3 and that the cooling rate is fast enough for a formation of the classical upper-bainitic structure in the HZ regions

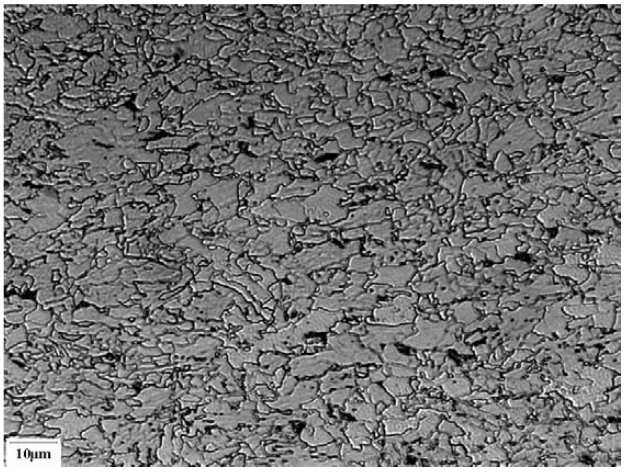

Figure 7: Base-metal microstructure of the X80 API-grade steel
Slika 7: Mikrostruktura osnovnega jekla X80 API

during the FSW process. As mentioned above, the bainitic structures of the HZs in different regions of the weld zone vary depending on the peak temperature and the strain rate on the AS of the weld zone during the FSW process. The SZ and the near-hard-zone (NHZ) microstructures display coarser bainitic structures and the bainite-lath boundaries in these bainitic structures are not as thin, straight and parallel as in the HZ regions (deformed lath bainite). Also, the SZ and NHZ have the polygonal ferrites distributed in a random manner and some martensite/austenite (M/A) islands are scattered throughout the coarse bainitic matrix. This microstructure is called granular bainite. It is formed at a slower cooling rate than the upper bainite.[21] The HAZ and the outer heat-affected zone (OHAZ) do not have a lath-bainitic microstructure. The elongated ferrite grains in the BM recrystallize and change into equiaxed polygonal ferrites in the HAZ, partially also in the OHAZ, during the FSW process. It is possible to say that the temperature in the HAZ was sufficient to cause a significant coarsening and a spheroidization of the carbides. The effective grain sizes of the HAZ, OHAZ and BM characterized with the EBSD analysis are 4.16 µm, 5.89 µm and 6.09 µm, respectively.

It is well-known that the bainitic microstructures in the weld zone are crucial for the post-weld properties. Therefore, a characterization of the bainitic structures needs to be done acquiring quantitative data in the weld zone for the FSWed X80 steel. It is known that bainite is a microstructure made up of packets of parallel, low-misorientation ferritic laths, which exhibit the same crystallographic orientation in the so-called morphological packets. Bainite packets are separated by high-angle boundaries, defined as the misorientation angles higher than 15°. Bainite-packet and lath size measurements of a bainite microstructure can be made from an IPF with an IQ map and a misorientation profile. An example of these measurements can be seen in **Figure 8**; the misorientation curve exhibits seven peaks, whose misorientation angles are higher than 15°. It shows six packets existing along this trace line. In short, the bainite packet size is the distance between the misorientation angles higher than 15°. Similarly, the bainite-lath size measurement can be made from an IPF with an IQ map and an IQ value curve (**Figure 8**); the lath boundaries

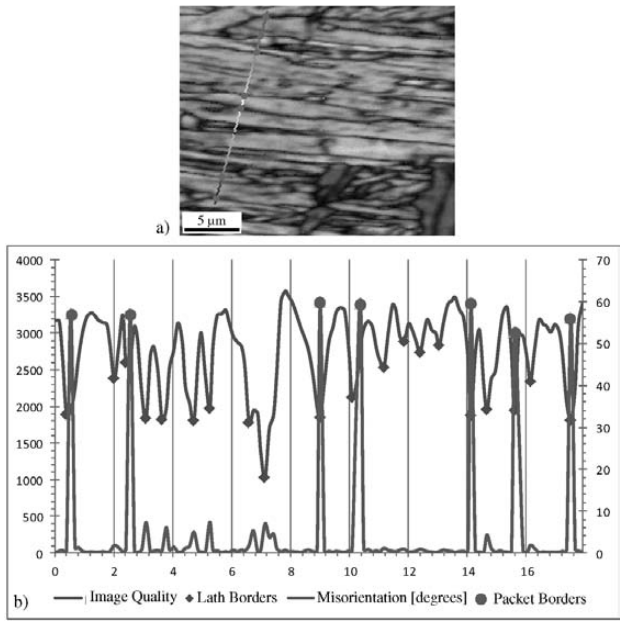

Figure 8: Bainite packet/lath size measurement: a) IPF with an IQ map with a trace line across the bainite microstructure; b) misorientation profile
Slika 8: Merjenje velikosti bainitnega sestava in bainitnih lat: a) IPF z IQ-področjem s sledovi linije preko bainitne mikrostrukture; b) profil razlike v kristalografski orientaciji

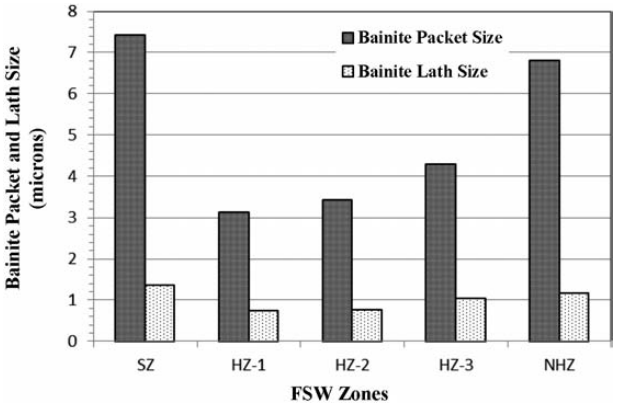

Figure 9: Bainite packet and lath sizes in different FSW zones
Slika 9: Velikost bainitnega sestava in bainitnih lat v različnih področjih FSW

Table 2: Bainite packet and lath sizes in different FSW zones
Tabela 2: Velikost bainitnega sestava in bainitnih lat v različnih področjih FSW

Weld zone	SZ	HZ-1	HZ-2	HZ-3	NHZ
Bainite packet size (µm)	7.42	3.14	3.43	4.29	6.80
Bainite lath size (µm)	1.35	0.73	0.76	1.05	1.16

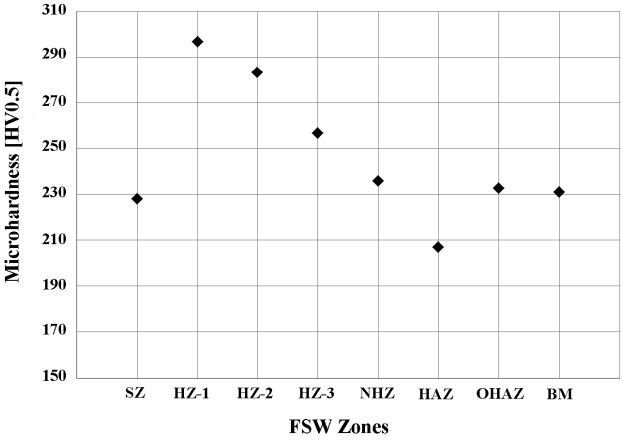

Figure 10: Microhardness profile in the weld zone of the FSW sample (the hardness values were obtained in the zones indicated with the arrows in **Figure 6**)

Slika 10: Profil mikrotrdote v področju zvara v vzorcih FSW (vrednosti trdote so bile izmerjene na področjih, označenih s puščico na **sliki 6**)

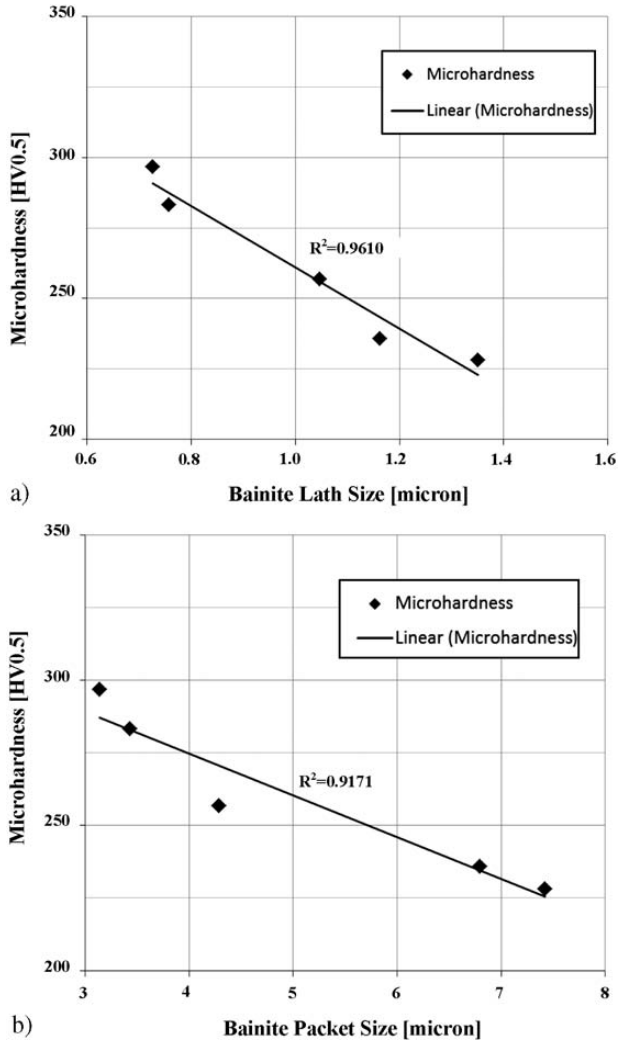

Figure 11: a) Bainite lath and b) bainite packet size versus microhardness in the FSW sample

Slika 11: a) Latasti bainit in b) velikost bainitnega sestava v odvisnosti od mikrotrdote v FSW-vzorcu

have a lower IQ value and so the lath size is the distance between the lower peaks of these quantities. The measurements were made at 15 locations on each zone to acquire statistical data of the bainite-lath and packet sizes in the weld-zone microstructures, using crystallographic data on the IPF with the IQ maps shown in **Figure 6**. The obtained results from the quantitative measurements can be seen in **Table 2** and **Figure 9**. As expected, the HZ regions have finer bainitic microstructures and GBs showing misorientations of 0.7–15° in the HZ regions, particularly in the HZ-1 and HZ-2 regions; their lath-bainitic structures are finer than those in the other zones (**Figure 6**). Bainite-lath and packet sizes of the HZ regions in different regions of the weld zone vary depending on the heat input and strain rate during the FSW process. The SZ and NHZ have coarse bainitic microstructures.

The hardness values in different regions of the weld zone of the FSW sample, depending on their microstructures, can be seen in **Figure 10**. Essentially, the hardness in the weld zone varies depending on the bainitic structures. As can also be seen in **Figure 11**, there is a direct relationship between the post-weld bainitic structures and the hardness values in the weld zone: the hardness increases almost linearly with the decreasing bainite-lath and packet size.

The TEM images of the SZ and HZ microstructures of the FSW sample are shown in **Figure 12**. The microstructure in the SZ is complicated, including differently shaped ferrites, such as non-equiaxial and interwoven, partially parallel lathy ferrites with high-density dislocations and coarse, dark phases distributed intra-lath and along the lath boundaries (**Figures 12a** to **12c**). There are also ultrafine particles inside the laths or among the laths. A fairly high dislocation density in this matrix is an essential characteristic of the intermediate transformation products[22] that form with a transformation mode between ferrite and martensite. The dark phases are M/A constituents or retained austenite.[23] As mentioned above, such a ferrite matrix is typically found in granular bainite. The formation of M/A constituents may be attributed to the partitioning of carbon during the transformation to bainite and the post-transformation of carbon-enriched austenite. An M/A constituent is a kind of a brittle mixture, its size and shape have a great effect on the toughness of steel. An M/A constituent converging to a block is beneficial to the improvement of the toughness compared with an M/A strip.[24] Thin M/A strips are observed in the well-defined lath-boundary locations in the HZ microstructure (**Figures 12d** and **12e**). It may be expected from the HZ region to exhibit a lower toughness than the SZ region since the HZ has more M/A strips.

Also, as can be seen in the TEM images, the widths of the bainite laths in the HZ are less than 1 μm, whereas the widths of the laths in the SZ are more than 1 μm. It is

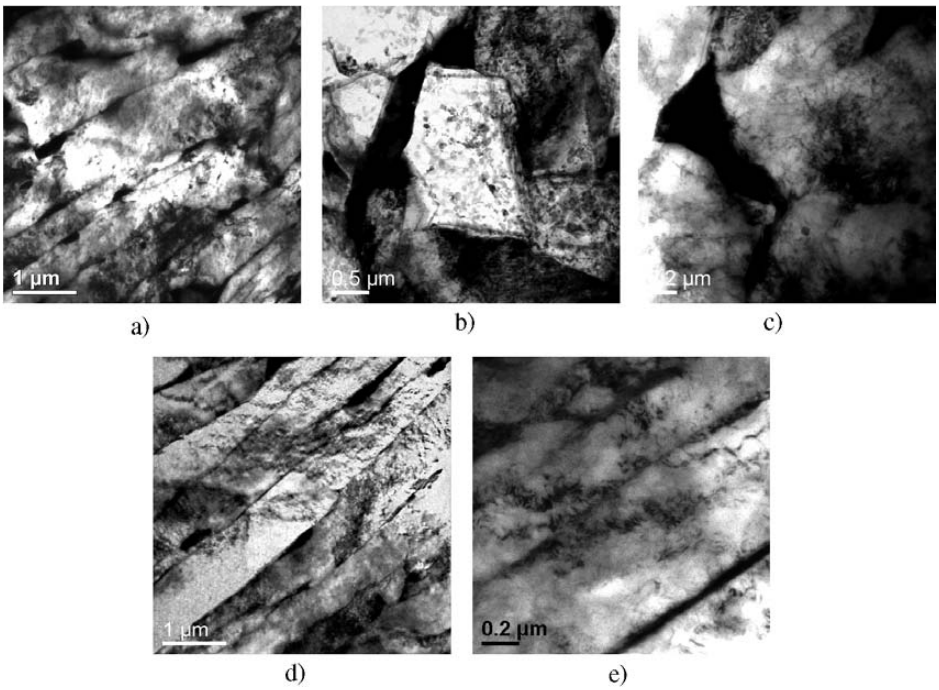

Figure 12: TEM micrographs of: a), b), c) the SZ region and d), e) the HZ-1 region of the FSW sample
Slika 12: TEM-posnetki: a), b), c) področja SZ in d), e) področja HZ-1v FSW-vzorcu

clear that this is the reason for the increased hardness of the HZ region (**Figures 11** and **12**).

4 CONCLUSIONS

The morphology of the weld zone, especially the quantitative microstructural characterization of bainitic structures, and the relationship between post-weld bainitic structures and the hardness at the weld zone of the friction-stir welded X80 API-grade pipe-line steel have been investigated in this study. In the FSWed X80 steel, the frictional heat and plastic flow create a granular bainitic structure in the stir zone, the classical lath-like upper bainitic structure in the hard zone, and a recrystallized equiaxed polygonal ferritic structure in the heat-affected zone. The maximum hardness was observed in the classical upper bainitic microstructure in the hard zone. The lowest hardness was associated with the heat-affected zone. The hardness values in the weld zone vary depending on the bainitic structure. A direct relationship between the post-weld bainitic structures and the hardness values in the weld zone has been determined: the hardness increases almost linearly with the decreasing bainite-lath and packet sizes.

Acknowledgments

The author is grateful to Prof. T. W. Nelson for providing the friction-stir research-laboratory facilities and Dr. J. Farrer for technical assistance at the Brigham Young University. The author also acknowledges the support provided by the Science Fellowships and Grant Programmes Department (BIDEB) of the Scientific and Technological Research Council of Turkey (TUBITAK).

5 REFERENCES

[1] Y. H. Zhao, S. B. Lin, L. Wu, F. X. Qu, Mater Lett., 59 (**2005**), 2948–2952
[2] N. Rajamanickam, V. Balusamy, Indian J Eng Mater Sci., 15 (**2008**), 293–299
[3] W. M. Thomas, E. D. Nicholas, J. C. Needham, M. G. Church, P. Templesmith, C. J. Dawes, GB Patent Application No. 9125978.9, 1991
[4] S. R. Ren, Z. Y. Ma, L. Q. Chen, Scr Mater., 56 (**2007**), 69–72
[5] R. S. Mishra, Z. Y. Ma, I. Charit, Mater Sci Eng., A 341 (**2003**) 1–2, 307–310
[6] H. Aydin, A. Bayram, U. Esme, Y. Kazancoglu, O. Güven, Mater. Tehnol., 44 (**2010**) 4, 205–211
[7] S. J. Barnes, A. R. Bhatti, A. Steuwer, R. Johnson, J. Altenkirch, P. J. Withers, Metall Mater Trans., A 43 (**2012**) 7, 2342–2355
[8] D. Forrest, J. Nguyen, M. Posada, J. DeLoach, D. Boyce, J. Cho, P. Dawson, Simulation of HSLA-65 Friction Stir Welding, 7th International Conference on Trends in Welding Research, Pine Mountain, 2006, 279–286
[9] S. Jindal, R. Chhibber, N. Mehta, Adv Mat Res., 365 (**2011**), 44–49
[10] L. Wei, T. W. Nelson, Characterization of microstructures and transformation behavior in friction stir welded HSLA-65, Trends in Welding Research, Proc. of the 8th Inter Con., Pine Mountain, 2008, 391–397
[11] L. Wei, T. W. Nelson, Weld J., 90 (**2011**), 95–101
[12] P. J. Konkol, M. F. Mruczek, Weld J., 86 (**2007**) 7, 187–195
[13] D. P. Field, T. W. Nelson, Y. Hovanski, K. V. Jata, Metall Mater Trans A, 32 (**2001**), 2869–2877
[14] P. S. Pao, R. W. Fonda, H. N. Jones, C. R. Feng, D. W. Moon, Friction stir welding of HSLA-65 steel, Friction Stir Welding and Processing, IV (**2007**), 243–252

[15] H. Farhat, I. N. A. Oguocha, Effect of welding speed on weld quality and microstructure of tandem submerged arc welded X80 pipeline steel, Materials Science & Technology Conference and Exhibition, Pittsburg, 2009, 2457–2468

[16] A. Ozekcin, H. W. Jin, J. Y. Koo, N. V. Bangaru, R. Ayer, Int J Offshore Polar Eng., 14 (**2004**) 4, 284–288

[17] T. F. A. Santos, T. F. C. Hermenegildo, C. R. M. Afonso, R. R. Marinho, M. T. P. Paes, A. J. Ramirez, Eng Fract Mech., 77 (**2010**), 2937–2945

[18] J. Defalco, R. Steel, Weld J., 88 (**2009**) 5, 44–48

[19] http://www.mtiwelding.com/files/FSW_RM2_vWeb.pdf

[20] http://fsrl.byu.edu/presentations/Dual%20Phase%20Steel.pdf

[21] S. K. Dhua, D. Mukerjee, D. S. Sarma, Metall Mater Trans A, 34 (**2003**), 2493–2504

[22] J. L. Lee, M. H. Hon, G. H. J. Cheng, J Mater Sci., 22 (**1987**), 2767–2777

[23] C. Xu, K. Shi, Y. Zhou, X. Li, Y. Liu, H. Wang, Trans Jpn Weld Res Inst., Special Issue on Welding Science and Engineering, (**2011**), 51–54

[24] J. Niu, L. Qi, Y. Liu, L. Ma, Y. Feng, J. Zhang, Trans Nonferrous Met Soc China, 19 (**2009**), 573–578